

# A Spatio-temporal Model-based Statistical Approach to Detect Evolving Multiple Sclerosis Lesions

D. Rey J. Stoeckel G. Malandain N. Ayache  
Epidaure Project  
INRIA, 2004 route des lucioles BP 93  
Sophia Antipolis, 06902 Sophia Antipolis Cedex. FRANCE.

## Abstract

*The effects of new treatments need to be assessed: in the case of multiple sclerosis it is possible to measure those effects by studying temporal lesions' evolutions in time series of MRI. But it is a laborious task to manually analyze such sets of images. This article proposes a new method to statistically analyze a series of T2-weighted MRI of a patient with multiple sclerosis lesions taking both temporal and spatial coherence into account. The main idea of the method is to fit a temporal parametric model of intensity evolution on each voxel of the series; these estimations give different parameter values in the case of normal and pathological areas. A statistical inference stage makes it possible to determine significant sets of connected voxels corresponding to pathological evolving areas. The significancy is estimated using permutations. Promising results show the feasibility of our approach. On our data sets the evolving lesions were detected and their temporal behavior could be quantified.*

## 1 Introduction

### 1.1 Medical Motivation: a Retrospective Clinical Analysis

Multiple sclerosis [1] is a progressive disease with evolving lesions over time. Lesions appear in the central nervous system: encephalon -and especially white matter-, spinal cord and optic nerves. Usually lesions are due to a demyelination with a replacement of cerebro-spinal fluid instead of myelin. There is a natural process of healing: a typical lesion expands to a maximum and then shrinks thanks to remyelination. Unfortunately this healing process is limited and rarefies over time.

MRI scans make it possible to confirm the diagnosis at the beginning of multiple sclerosis [2, 3, 4]: hypersignals in T2 weighted or Proton Density images show lesions but do not differentiate oedema, demyelination, sclerosis and eventually necrosis; T1 weighted images show necrosis, and T1 images with gadolinium injections show the active de-

myelinizing areas [5, 6]. Some automatic methods make it possible to find lesions based one temporal exam (e.g. [7, 8]).

Moreover Guttmann *et al.* [9] show that MR scans make it also possible to do the follow-up of a patient with multiple sclerosis. In this case a time series of 3D images of a patient is usually acquired from the same modality and with a specific protocol to have similar properties: field of view, image size, voxel size, etc.

On the one hand it is possible to compare two images to know where there are differences, typically between the last and the previous exam. Such a comparison makes it possible to find if lesions have grown, shrunk or remained stationary since the previous exam. This is typically a short-term analysis that helps on the current diagnosis of a patient. Detection and quantification methods have already been developed in this case [10, 11, 12, 13]. On the other hand we may want to achieve a retrospective analysis on a whole set of images to find the moments when evolutions occur, especially to know the effect of a treatment over a long-period. This is a long-term analysis that takes into account all the images of a patient over time (for instance a year as in this report). Previous work allows an automatic detection based on the temporal profiles of voxel intensities over time (Figure 1 shows the profile of a temporal evolving point in a lesion from a set of 3D T2-weighted MRI): Gerig *et al.* [14] takes only into account the temporal information at each voxel; Welti *et al.* extends this work by adding a spatio-temporal post-processing to the previous algorithm; some recent work directly takes the spatio-temporal aspect into account with a statistical methodology based on an average evolving lesion model [15, 16].

This paper presents a new statistical method for a retrospective analysis based on the temporal evolution of voxel intensities where both temporal and spatial coherences are intrinsically taken into account. Compared to Rey *et al.* [15] this new method requires less stringent assumptions on the statistics of the images and does not require a fixed model of lesion evolution. It does not only provide information about the presence of lesions, but it also gives quanti-

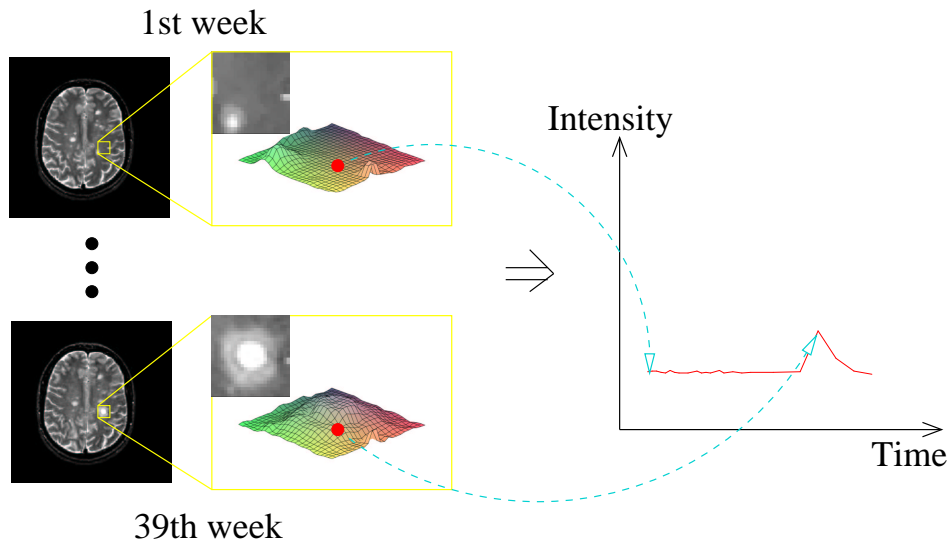


Figure 1: A “profile of intensity” shows the intensity of the same anatomical point of 3D images over time.

tative measurements on the evolutionary process in each of them (rising time, decreasing time, lesion amplitude, etc.).

## 1.2 Overview of the model-based statistical method

This section gives a brief overview of our method. It consists in three main parts which will be described in the next sections:

- **Pre-processings:** the temporal series of images needs pre-processing; the images must be realigned to establish the anatomical correspondence between the images, and the temporal bias must be corrected to enforce the intensity scale of each image to be the same (see section 2).
- **Parametric model:** a parametric model of intensity profiles over time is fitted on each voxel. This model is chosen such as to describe the intensity evolution of a voxel attached to an evolving lesion. In the sequel, we call such a voxel **ELV** which stands for **Evolving Lesion Voxel**. We only consider evolving lesions which both expand and shrink within the limits of the time series.
- **Statistical inference:** a statistical analysis is done (see section 4) to detect clusters of voxels which significantly correspond to evolving pathological areas. If there are several connected voxels with a significant pathological profile, the probability of this cluster to correspond to a pathological evolving area is larger than for an isolated voxel.

Thus our method takes into account both temporal and spatial coherence of the evolving pathological areas: the temporal coherence is enforced through the use of a parametric model of voxel intensity profile, and the statistical analysis method takes the spatial coherence into account by considering clusters of voxels. Please note that the analysis takes place in 3D.

## 2 Pre-processings

### 2.1 Rigid registration

In the case of a study over a long-period, the patient does not have exactly the same position in the imaging machine for each exam. Therefore a point with the same coordinates in two images taken at different moments does not correspond to the same anatomical point. A first stage of data realignment is thus required: we have used a geometrical method based on matching 3D extremal points of the crest lines [17] and a cubic spline interpolation to resample all the images of the series with the first one. Then with sub-voxel precision [18] a point at given coordinates in the images of the series now corresponds to the same anatomical point (Figure 4). It is also possible to align images with an iconic method -based on the intensity- [19], but geometrical approaches are more adapted to intra-patient, mono-modal images with local intensity differences (e.g. due to evolving lesions).

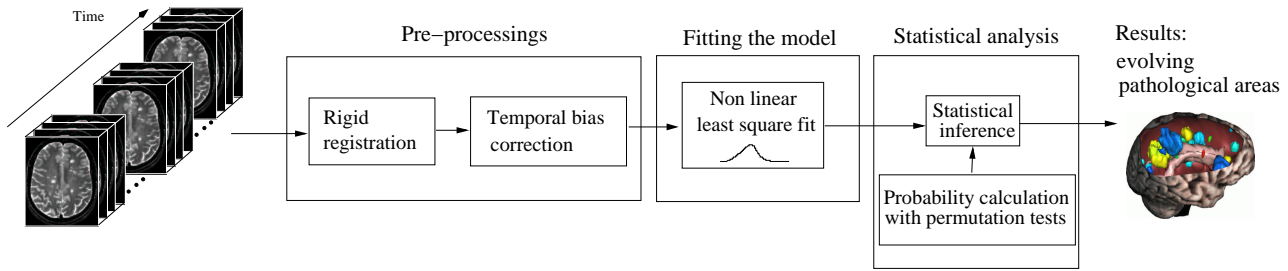


Figure 2: Overview of the three main stages which allow to find the significant evolving pathological areas in a set of images.

## 2.2 Spatial bias correction

Magnetic field inhomogeneities in MRI cause spatial bias which is problematic in most MRI-based analyses. Methods to correct this spatial bias have been developed [20, 21]. In the case of MRI of the brain, the shape of the bias is mainly defined by the shape of the patient’s head and by the type of MR machine [22]. In our case of intra-patient analysis with T2-weighted images acquired on the same machine with a fixed protocol, the spatial bias has almost the same shape in the scans of the whole series [22]. The temporal intensity profiles are analyzed locally and thus it is reasonable to omit this pre-processing in our case. Moreover experiments with spatial bias correction did not seem to improve the results.

## 2.3 Temporal bias correction

Image intensities are not directly comparable because MRI scans intensity scale is not absolute as e.g. in CT scans. In two images acquired at different moments the same material might have different intensities depending on the machine calibration, on the operator, and on several other external parameters. Therefore intensity profiles over time are biased. Thus a pre-processing stage consisting in the temporal bias correction of the MRI intensities over time is required.

The shape of the joint histogram between two identical images is a diagonal straight line whereas this shape between two different registered images of our series is an elongated cloud which is not oriented along the first diagonal (Figure 3-c). The shape of the joint histogram can be modelled as an affine function:  $I_2 = A(I_1) = a \times I_1 + b$ . Where  $I_1$  and  $I_2$  are respectively the intensity of the first and the second image. The parameters of  $A$  are found with a robust orthogonal least square estimation. The correction of the global intensity difference between two images is obtained by applying  $A$  to the first image. Figure 3 shows results of the intensity correction with the corresponding joint histograms.

Those pre-processing stages of alignment and temporal intensity correction give a series of comparable images for a voxel analysis over time (Figure 4).

## 3 Parametric Model of Evolving Voxels in MS Lesions

The method aims at detecting the ELVs which have a typical intensity profile. This section presents a parametric model of ELV which has to take into account the variability of ELV profiles.

### 3.1 Parametric Model

Considering the shape of each profile, a typical curve of evolving pathological point over time is composed of a rising part and a decreasing part (figure 5-a shows ELV profiles extracted from different evolving lesions). Furthermore the curve is generally asymmetric. Thus we decided to fit a kind of asymmetric Gaussian with five free parameters: amplitude, mean, rising width, decreasing width and vertical offset. The model is

$$f(x) = p_1 e^{-g(x-p_2)^2} + p_5 \quad (1)$$

with

$$g(x) = p_3(x + \sqrt{1+x^2}) + p_4(x - \sqrt{1+x^2}) \quad (2)$$

Figure 5-b shows an example of the model curve. This model is fitted for each voxel of the series of images .

### 3.2 Parameter Estimation

The temporal resolution of our time series is relatively low compared to the speed of evolution of the pathological process. For most of the lesions, the time between the appearance and disappearance is around eight weeks whereas the time interval between images vary from one to six weeks.

Our model (section 5) has been chosen to fit evolving lesions taking into account their physical quantities such as the amplitude, the rising width or the decreasing width. However because of the low temporal resolution, it is not possible to estimate all these physical quantities at the same

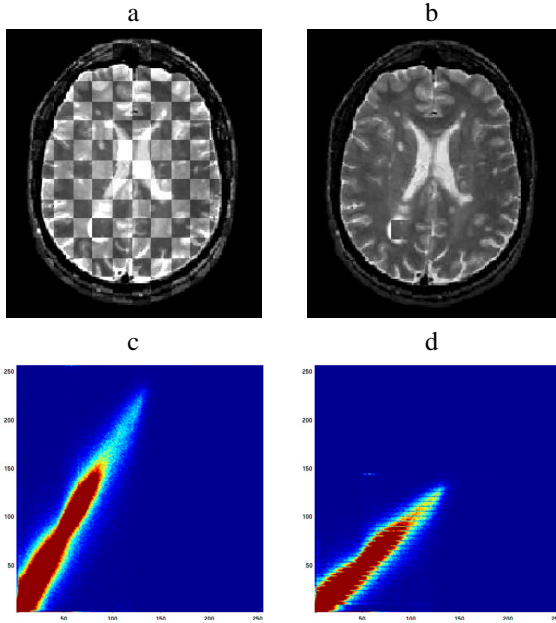


Figure 3: The 2 images on the left are displayed as a checkerboard with an alternation of cubes of data of 2 images: a) image 1 with registered image 2. b) image 1 with registered and corrected image 2; it is difficult to distinguish the alternating cubes excepted in the areas where lesions have evolved. The 2 images on the right are the corresponding joint-histograms: c) joint-histogram of registered image 2 intensity vs image 1 intensity. d) joint-histogram of registered and corrected image 2 intensity vs image 1 intensity.

time on a single temporal profile. We chose to fix the rising width and decreasing width of the model prior to the parameter estimation to cope with this problem. The values of these parameters are estimated globally on a normalized training set of many ELV profiles. Fixing these parameters does not turn out to be very constraining; all ELV profiles of the training set have about the same width at half maximum, e.g.  $\overline{FWHM} = 6.3 \text{ weeks}$  and  $\sigma_{FWHM} = 3.5 \text{ weeks}$ .

The parametric model is fitted in the least square sense using Powell’s quadratically convergent method [23]. Please note that for computational issues we have squared the amplitude parameter to improve convergence. Moreover, the model is first fitted to a temporally smoothed version of each profile, this is used to initialize the minimization using the original profile.

## 4 Statistical Analysis

In our method the ELVs should correspond to the areas where the values of the fitted model parameters clearly indicate an evolving pathological behavior. To take into account

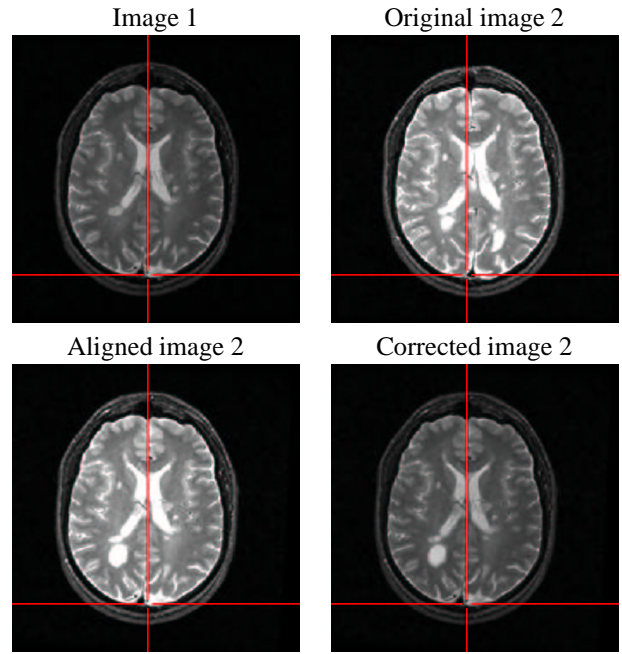


Figure 4: Pre-processing stages of alignment and intensity correction give a series of comparable images in the purpose of a voxel analysis over time. Image 2 has been registered and corrected with respect to image 1.

the spatial aspect of the lesions we are interested not just in the single voxels but in the areas which have a higher than normal amplitude parameter  $h$  (Figure 6).

### 4.1 Statistical Inference

We define these regions by thresholding the  $h$ -image at an appropriate value  $t$  (see below), inducing clusters of voxels. Clusters are the sets of connected voxels with suprathreshold values. We can assess the significance of clusters based on their size. The null hypothesis is fulfilled when there are no evolving lesions in the image series. In other words, the null distribution is the distribution of cluster sizes when no evolving pathological areas are present. Based on the null distribution, we consider as significant those clusters whose size is such that they have a probability to occur under the null hypothesis lower than the critical value  $\alpha$ .

The threshold  $t$  is chosen appropriately in order to detect meaningful clusters. Fortunately the value of the threshold does not influence the validity of our statistics, yet it does influence the sensitivity of our analysis.

### 4.2 Cluster size probability distribution

In our case, the cluster size probability distribution is not known analytically; in some other cases under stringent hy-

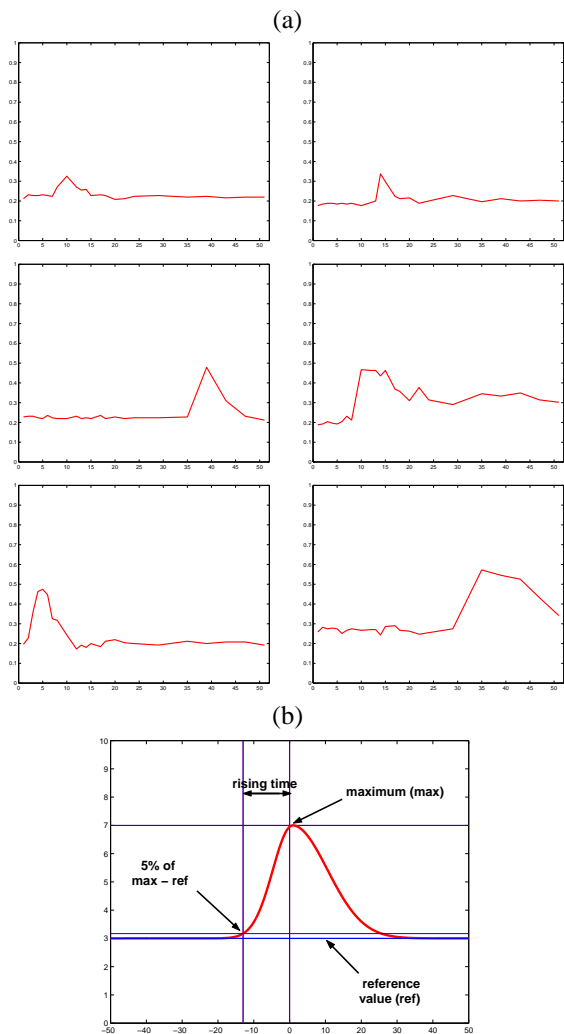


Figure 5: *a) Typical curves of evolving pathological voxels over time are composed of a rising part and a decreasing part. b) An instance of our model of evolving profile with five parameters.*

potheses some analytical approximations can be found (e.g. cluster size distribution in random Gaussian fields [24, 15]).

In our case we estimate the cluster size distribution using permutations (see section 4.2). The exchangeability of the images is a sufficient condition for the permutation test to be exact [25]. The images of the series are exchangeable if they can be considered to be independent observations and identically distributed ([26] p. 18). We can reasonably assume the independence of the observation of the images over time: the time between two acquisitions is large enough to have no temporal correlation of the noise between them. The noise is assumed to have the same distribution over time because the images of one series are acquired with the same imaging machine.

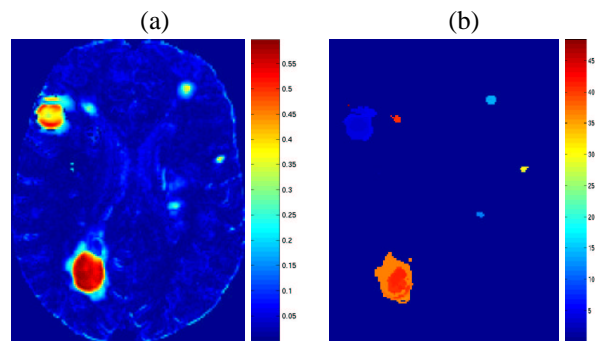


Figure 6: *Estimated parameter results for data set  $S_1$  (see section 5). Only one axial slice of the 3D volume is shown. (a) h-image. (b) Time of maximum intensity value of each profile on the significant clusters (in weeks).*

Estimating the cluster size probability distribution is done with the following steps [27]:

- Randomly modify the order of the images of the series, thus reassigning each image of the time series to a different time step, apply the identical permutation at each voxel to preserve the spatial correlation structure of the individual images [28].
- fit the parametric model to this permuted time series and apply the threshold  $t$ .
- measure the size of each suprathreshold cluster.
- repeat the previous three steps  $n$  times and pool the resulting cluster size measures to sample the permutation distribution (see e.g. figure 7).

$n$  is determined in such a way as to make the process tractable computationally and in the same time have a good approximation of the probability density distribution. In our case where we pool all the cluster sizes of each permutation it can be assumed that  $n \approx 10$  is sufficient [29, 27].

## 5 Materials

In this article we show results on a time series  $S_1$  of T2-weighted MRI provided by Dr. Charles Guttman and Dr. Ron Kikinis, Brigham and Women's Hospital, and Harvard Medical School. Each image has a size of  $256 \times 256 \times 54$  and a voxel size of  $0.9375 \times 0.9375 \times 3.0 \text{ mm}^3$ . There are 24 time points over one year with a temporal interval between two images of the series which varies from one week to six weeks with an average of two weeks.

We conducted some preliminary experiments on a set  $S_2$  of 10 T2-weighted MRI acquired every month, with a size of  $256 \times 256 \times 44$  and a voxel size of  $0.9 \times 0.9 \times 3.0 \text{ mm}^3$ .

The geometric distortions in these images required an additional stage of affine registration. These were provided by Dr. Massimo Filippi and Dr. Marco Rovaris<sup>1</sup> as part of a larger collaboration between QuantifiCare<sup>2</sup>, the neuroscience department of the San Raffaele Hospital in Milan and the Epidaure project at INRIA.

## 6 Results

The experiments conducted in this section aim at verifying the feasibility of our approach. Unfortunately no ground truth for our image series was available. Thus we assess the results based on visual observation.

We applied the above described methodology to both image series. Due to the limited space of this article the figures only depict results on series  $S_1$ . As mentioned above, only the lesions of which the rising time as well as the decreasing time fall within the limits of the time series are considered.

Visual inspection showed that all evolving lesions in series  $S_1$  were detected. Figure 8 shows some image slices with detected lesions ( $t = 0.2$ ,  $\alpha = 0.01$ , see section 4.1). The results of the permutations are found in figure 7. Based on this histogram, we can calculate by integration that clusters of size larger than ten voxels are to be considered significant.

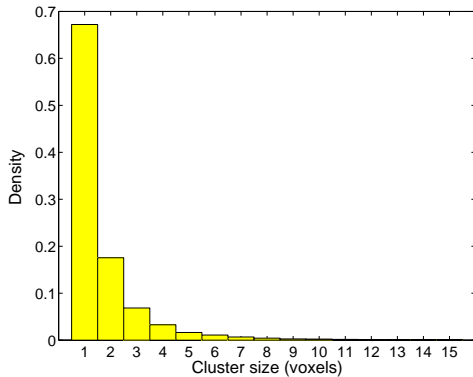


Figure 7: *Permutation distribution for the size of suprathreshold voxel clusters for series  $S_1$  and  $t = 0.2$ .*

Analysis of series  $S_2$  proved to be more difficult due to geometric distortions of some images. However also in this case all lesions were detected ( $t = 0.1$ ,  $\alpha = 0.01$ , i.e. cluster sizes above thirteen voxels are significant). Some sulci were detected as well due to local misregistration.

<sup>1</sup>neuroscience department, Ospedale San Raffaele, Milano

<sup>2</sup><http://www.quantificare.com/>

## 7 Discussion

In practice, time series have a low temporal resolution essentially for the convenience of the patient. We showed that by fixing some parameters of our model we obtain meaningful results even on this type of series. When acquiring the images one should take into account the speed of evolution when choosing the time interval between the images. Furthermore we need a minimal number of images for being able to deduct meaningful statistical results.

Our method can be extended by using models that can describe lesions which only rise, only decrease, or even lesions that appear multiple times at the same position.

If the spatial bias is additive, the statistical analysis of the amplitude is still correct. However, if the spatial bias can not reasonably be approximated as being additive, the bias should be corrected to obtain the same detection sensitivity for all voxel positions.

The sensitivity of our method depends on the value of the threshold  $t$ . The sensitivity could be optimized by testing different threshold values on a different dataset, having the same distributions as the dataset one wishes to analyze. In most cases, such datasets are not available. Therefore, the  $t$  threshold is usually fixed arbitrarily prior to the analysis to prevent a bias on the resulting statistics.

As described in section 6, some false positives are detected with our approach due to local misregistration around the sulci. MS lesions in the brain are located in the white matter. The use of a white matter mask [30] will prevent false positive detection in other brain areas.

Quantitative comparisons allow to test the validity of our approach 1) by comparing manual and automatic segmentations and 2) by correlating clinical signs with results of our automatic analysis. In the case of evolving lesions detection in MRI, the validation is a long and difficult task because it is hard to precisely define manually ground truth in the image series. An alternative way to partially validate algorithms in this case is to use synthetic datasets [14]. However this still depends on the choice of the simulation model of the incompletely known evolving process.

## 8 Conclusion

In this article we presented a new method that aims at retrospectively finding coherent areas corresponding to evolving multiple sclerosis lesions of a patient in a time series of MRI scans acquired over a long time period. First we proposed a parametric model of temporal evolution of multiple sclerosis lesions. Then we explained how we used our model and statistical inference to detect areas of significant pathological evolution. Permutation tests allow to choose the test statistic (for instance suprathreshold cluster size) freely even

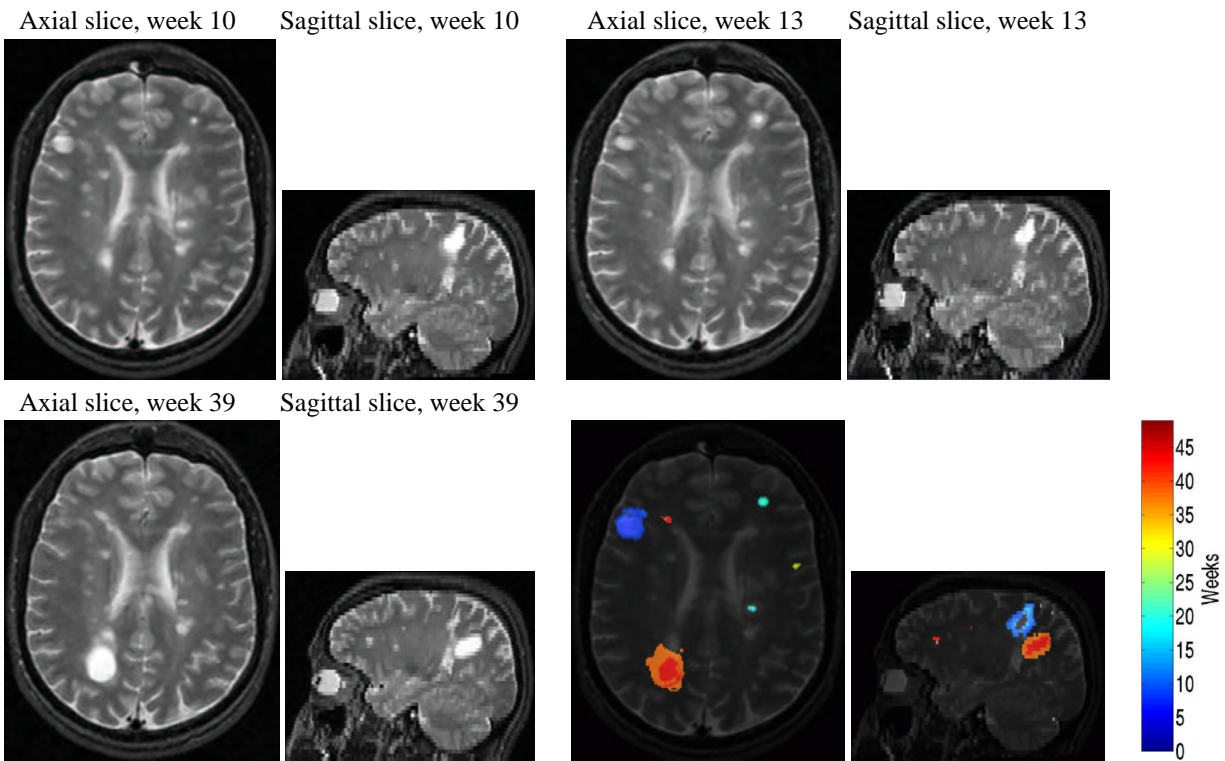


Figure 8: Results for data set  $S_1$ . First, three image series samples at weeks 10, 13 and 39 are shown. The lower right shows evolving lesions with a color related to the time of the maximum intensity occurrence superimposed on an image of the series. Lesions with no significant evolution are not detected.

if no analytical probability distributions are known. The results show our approach to be able to provide clinicians with quantitative information about evolving areas.

This type of method might be used for other pathologies with evolving areas by choosing an appropriate model for the evolving process.

## Acknowledgments

We would like to thank Dr. Charles Guttmann and Dr. Ron Kikinis, Brigham and Women’s Hospital, and Harvard Medical School, who provided us with a database of multiple sclerosis images.

Many thanks to Dr. Massimo Filippi and Dr. Marco Rovaris, neuroscience department, Ospedale San Raffaele (Milano), who provided us with a T2-weighted MRI series of a patient with MS lesions.

We would like to thank Jean-Philippe Thirion and Bruno Vassel, QuantifiCare, France. Many thanks to Pascal Cachier for fruitful discussions about the model of evolving lesions.

Finally we would like to thank Chet Baker for his perma-

nent support.

This work was partially supported by ADER PACA.

## References

- [1] O. Lyon-Caen and M. Clanet. *La sclérose en plaques*. John Libbey, 1998.
- [2] C. R. G. Guttmann, S. S. Ahn, L. Hsu, R. Kikinis, and F. A. Jolesz. The Evolution of Multiple Sclerosis Lesions on Serial MR. *American Journal of NeuroRadiology*, 16:1481–1491, August 1995.
- [3] C. J. Wallace, P. Seland, and T. Chen Fong. Multiple Sclerosis: The Impact of MR Imaging. *AJR*, 158:849–857, April 1992.
- [4] Th. Duprez, C.J.M. Sindic, and Ph. Indekeu. Sequester-like appearance of a multiple sclerosis brain lesion on serial magnetic resonance images. *Acta neurol. belg.*, 99:202–206, 1999.
- [5] M. A. A. Van Walderveen, F. Barkhof, O. R. Hommes, C. H. Polman, H. Tobi, S. T. F. M. Frequin, and J. Valk. Correlating MRI and clinical disease activity in multiple sclerosis: relevance of hypointense lesions on short-TR/short-TE (T1-weighted) spin-echo images. *Neurology*, 45:1684–1690, September 1995.

- [6] L. Truyen, J. H. T. M. Van Waesberghe, M. A. A. Van Walderveen, B. W. Van Oosten, C. H. Polman, O. R. Hommes, H. J. A. Adèr, and F. Barkhof. Accumulation of hypointense lesions ("black holes") on T1 spin-echo MRI correlates with disease progression in multiple sclerosis. *Neurology*, 47:1469–1476, 1996.
- [7] A. Zijdenbos, R. Forghani, and A. Evans. Automatic Quantification of MS Lesions in 3D MRI Brain Data Sets: Validation of INSECT. In W. M. Wells, A. Colchester, and S. Delp, editors, *the First International Conference on Medical Image Computing and Computer-Assisted Intervention, MIC-CAI'98*, volume 1496 of *Lecture Notes in Computer Science*, pages 439–448, Boston, USA, October 1998.
- [8] K. Van Leemput, F. Maes, D. Vandermeulen, and P. Suetens. Automated Model-Based Tissue Classification of MR Images of the Brain. *IEEE Transactions on Medical Imaging*, 18(10):897–908, 1999.
- [9] C. R. G. Guttman, S. S. Ahn, L. Hsu, R. Kikinis, and F. A. Jolesz. Quantitative Follow-up of Patients With Multiple Sclerosis Using MRI: Reproducibility. *Journal of Magnetic Resonance Imaging*, 9:509–518, 1999.
- [10] D. Rey, G. Subsol, H. Delingette, and N. Ayache. Automatic Detection and Segmentation of Evolving Processes in 3D Medical Images: Application to Multiple Sclerosis. In A. Kuba, M. Sámal, and A. Todd-Pokropek, editors, *Information Processing in Medical Imaging, IPMI'99*, volume 1613 of *Lecture Notes in Computer Science*, pages 154–167, Visegrád, Hungary, June 1999. Springer.
- [11] D. Rey, C. Lebrun-Frénay, G. Malandain, S. Chanalet, N. Ayache, and M. Chatel. A New Method to Detect and Quantify Evolving MS Lesions by Mathematical Operators. In *American Academy of Neurology, 52nd Annual Meeting*, volume 54(7) of *Neurology (Supplement 3)*, page 123, San Diego, USA (Californy), May 2000.
- [12] L. Lemieux, U. C. Wiesmann, N. F. Moran, D. R. Fish, and S. D. Shorvon. The detection and significance of subtle changes in mixed-signal brain lesions by serial MRI scan matching and spatial normalization. *Medical Image Analysis*, 2(3):227–242, 1998.
- [13] J. P. Thirion and Calmon G. Deformation Analysis to Detect and Quantify Active Lesions in Three-Dimensional Medical Image Sequences. *IEEE Transactions on Medical Imaging*, 18(5):429–441, 1999.
- [14] G. Gerig, D. Welti, C. R. G. Guttman, A. C. F. Colchester, and G. Székely. Exploring the discrimination power of the time domain for segmentation and characterization of active lesions in serial MR data. *Medical Image Analysis*, 4(1):31–42, 2000.
- [15] D. Rey, J. Stoeckel, G. Malandain, and N. Ayache. Using SPM to Detect Evolving MS Lesions. In *Proc. of MIC-CAI'01*, LNCS, Utrecht, The Netherlands, October 2000. To be published.
- [16] D. Rey, J. Stoeckel, G. Malandain, and N. Ayache. Statistical analyses to detect evolving multiple sclerosis lesions in time series of 3d mri. Technical report, INRIA, 2001. In progress.
- [17] J. P. Thirion. New Feature Points Based on Geometric Invariants for 3D Image Registration. *International Journal of Computer Vision*, 18(2):121–137, May 1996.
- [18] X. Pennec and J. P. Thirion. A Framework for Uncertainty and Validation of 3D Registration Methods based on Points and Frames. *IJCV*, 25(3):203–229, 1997.
- [19] A. Roche, G. Malandain, and N. Ayache. Unifying Maximum Likelihood Approaches in Medical Image Registration. *International Journal of Imaging Systems and Technology (IJIST)*, 11:71–80, 2000.
- [20] K. Van Leemput, F. Maes, D. Vandermeulen, and P. Suetens. Automated Model-Based Bias Field Correction of MR Images of the Brain. *IEEE Transactions on Medical Imaging*, 18(10):885–896, 1999.
- [21] S. Prima. *Etude de la symétrie bilatérale en imagerie cérébrale volumique*. PhD thesis, Université de Paris XI, 2001.
- [22] J.G. Sled and B. Pike. Standing-Wave and RF Penetration Artifacts Caused by Elliptic Geometry: An Electrodynamics Analysis of MRI. *IEEE Transactions on Medical Imaging*, 17(4):653–662, 1998.
- [23] W.H. Press, S.A. Teukolsky, W.T. Vetterling, and B. P. Flannery. *Numerical Recipes. The Art of Scientific Computing*. Cambridge University Press, 2nd edition, 1997.
- [24] K.J. Worsley. Local maxima and the expected euler characteristic of excursion sets of  $\chi^2$ ,  $f$  and  $t$  fields. *Advances in Applied Probability*, 26:13–42, 1994.
- [25] E.L. Lehman. *Testing Statistical Hypotheses*. John Wiley and Sons, New York, 1986.
- [26] P. Good. *Permutation Tests. A Practical Guide to Resampling Methods for Testing Hypotheses*. Springer, 1993.
- [27] E.T. Bullmore, J. Suckling, S. Overmeyer, S. Rabe-Hesketh, E. Taylor, and M.J. Brammer. Global, Voxel, and Cluster Tests, by Theory and Permutation, for a Difference Between Two Groups of Structural MR Images of the Brain. *IEEE Transactions on Medical Imaging*, 18(1):32–42, January 1999.
- [28] S. Rabe-Hesketh, E.T. Bullmore, and M.J. Brammer. Analysis of Functional Magnetic Resonance Images. *Statistical Methods in Medical Research*, 6:215–237, 1997.
- [29] E.T. Bullmore, J. Suckling, and M.J. Brammer. In *Praise of Tedious Permutation*, volume 159 of *Lecture Notes in Statistics*, chapter 9, pages 183–200. Springer, 2001.
- [30] S. Warfield, J. Dengler, J. Zaers, C. Guttman, W. Gil, J. Etinger, J. Hiller, and R. Kikinis. Automatic identification of Grey Matter Structures from MRI to Improve the Segmentation of White Matter Lesions. *Journal of Image Guided Surgery*, 1(6):326–338, 1995.